PSFC/JA-11-31

Steady I-mode Plasmas in Alcator C-Mod

E. S. Marmar[a], A. Dominguez[a], M.J. Greenwald[a], N. Howard[a], A.E. Hubbard[a], J.W. Hughes[a], C. Kessel[b], B. LaBombard[a], B. Lipschultz[a], M.L. Reinke[a], J.E. Rice[a], P.B. Snyder[c], J.L. Terry[a], A.E. White[a], and D.G. Whyte[a]

[a]*MIT Plasma Science and Fusion Center, Cambridge MA 02139 USA*
[b]*Princeton Plasma Physics Laboratory, Princeton, NJ 08543 USA*
[c]*General Atomics, La Jolla, CA 92121 USA*

December, 2011

Plasma Science and Fusion Center
Massachusetts Institute of Technology
Cambridge MA 02139 USA

This work was supported by the U.S. Department of Energy, Grant No. DE-FC02-99ER54512-CMOD.

Steady I-mode Plasmas in Alcator C-Mod*

E. S. Marmar[a], A. Dominguez[a], M.J. Greenwald[a], N. Howard[a], A.E. Hubbard[a], J.W. Hughes[a], C. Kessel[b], B. LaBombard[a], B. Lipschultz[a], M.L. Reinke[a], J.E. Rice[a], P.B. Snyder[c], J.L. Terry[a], A.E. White[a], and D.G. Whyte[a]

[a]*MIT Plasma Science and Fusion Center, Cambridge MA 02139 USA*

[b]*Princeton Plasma Physics Laboratory, Princeton, NJ 08543 USA*

[c]*General Atomics, La Jolla, CA 92121 USA*

E-mail contact of main author: marmar@psfc.mit.edu

*Work supported by U.S. Department of Energy Office of Science, Fusion Energy Sciences

Abstract:

I-mode operation on the Alcator C-Mod tokamak combines a strong edge thermal transport barrier with L-mode levels of particle and impurity transport, allowing access to very high performance discharges with low pedestal collisionality, high central temperatures up to 9 keV, and without large ELMs or other intermittent edge instabilities. In recent experiments, C-Mod I-modes have been extended to quasi-steady-state. I-modes with normalized energy confinement quality factor H_98~1.0 to 1.2 can be maintained with input power up to nearly two times the threshold power, with the largest accessible range in closed divertor geometry at modest triangularity. Simple extrapolations at fixed field imply that ITER could access I-mode with available power, and stay in I-mode with alpha-dominant heating. Detailed pedestal fluctuation measurements reveal changes in the turbulence, with decreases in the power at some size scales and growth of a weakly coherent mode (WCM) (k_θ~1.5 cm^{-1}, $\delta f/f \sim .3$) which propagates in the electron diamagnetic direction in the plasma frame. The WCM, which has density, temperature and magnetic signatures, appears to play a key role in pedestal density and impurity regulation. Stability analysis shows that the typical I-mode pedestal is well away from the peeling-ballooning boundary.The distribution of divertor exhaust power depends on ion drift direction, with nearly equal power flows to the inner and outer strike points in single-null configurations.

I. INTRODUCTION

There is a significant need to find high confinement operational regimes in the tokamak which do not require intermittent edge instabilities to regulate particle and impurity transport across the edge transport barrier. In particular, the peak power loading from Edge Localized Modes (ELMs)[1], which usually are seen in the high performance H-mode regime[2], could be particularly problematic for next-step devices, including ITER[3], and for reactors, because of their potential to cause significant first-wall erosion in the divertor.[4,5] Several promising approaches to ELM elimination or mitigation are being pursued, including suppression with externally applied 3D

magnetic field perturbations[6,7], ELM pacing with small pellets[8], and ELM-free regimes including Quiescent H-mode (QH-mode)[9] and Enhanced D-Alpha H-mode (EDA H-mode)[10]. The I-mode regime[11-14] is another approach which combines several favorable characteristics: enhanced energy confinement with a strong thermal barrier near the last closed flux surface; little or no change in particle or impurity transport at the plasma edge, with L-mode like density profiles and global impurity confinement; no need for ELMs to regulate particle and impurity transport across the thermal barrier. There is no external momentum drive in these ICRF H-minority heated C-Mod plasmas. Easiest access to I-mode is found by operating in a single-null divertor configuration, with the ion ∇B/curvature drift in the so-called unfavorable direction for access to H-mode, away from the active X-point. I-mode has also been accessed on C-Mod with favorable drift, but the operational window in terms of input power between I- and H-mode is so far always observed to be small, whereas for unfavorable drift, I-mode has been accessed and maintained with nearly a factor of two increase in heating power, in some cases staying in I-mode for more than 10 energy confinement times with maximum available auxiliary power. Global energy confinement is significantly enhanced over L-mode, and comparable to H-mode, with $\tau_E/\tau_{ITER\text{-}H98,Y2} \leq 1.2$.

II. STATIONARY I-MODE PROPERTIES

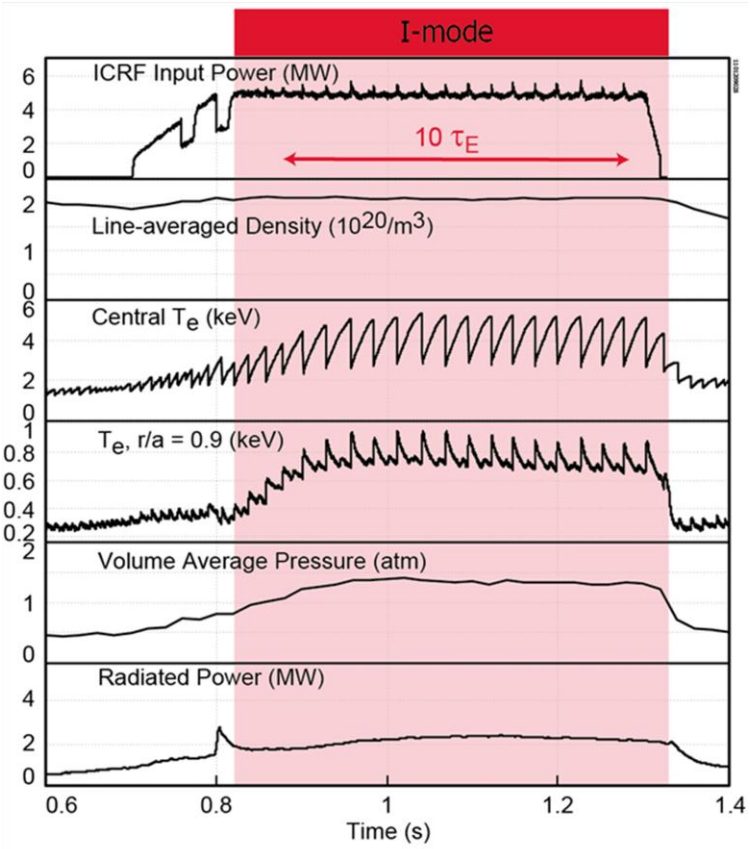

Fig. 1. Time histories for plasma parameters in a typical stationary I-mode discharge. The plasma current was 1.3 MA, the on-axis toroidal magnetic field was 5.6T, and q_{95}=3.2.

Time histories of plasma parameters for a typical stationary I-mode discharge are shown in Figure 1. For this case at I_p=1.3MA, B_φ=5.6T, and q_{95}=3.2, the divertor topology is upper single null, with $\mathbf{B}\times\nabla B$ away from the active X-point. The transition from L- to I-mode, as manifested by the strong increase in ∇T (both electrons and ions) near the plasma edge, occurs in this discharge just after t=0.8 s. The plasma density does not increase after the transition, and the density profile is also essentially unchanged from L-mode. As is also typical in I-mode, radiated power is well controlled. Global impurity confinement times, measured with trace calcium using the laser blow-off technique, are similar in I- and L-mode, about a factor of

5 shorter than in comparable EDA-H-mode plasmas[15]. In addition to keeping core intrinsic impurity levels down, this also allows for more aggressive low Z impurity gas seeding into I-mode discharges, enhancing SOL/divertor radiation, and thus reducing divertor heat loading near the strike points. Neon and/or nitrogen puffing is routinely used during I-mode operation on C-Mod. In addition, there is no need for recent boronization to achieve high performance I-mode conditions; this is very different from the H-mode experience on C-Mod, where boronization is required to keep core radiation, particularly from molybdenum, within acceptable limits.[16]

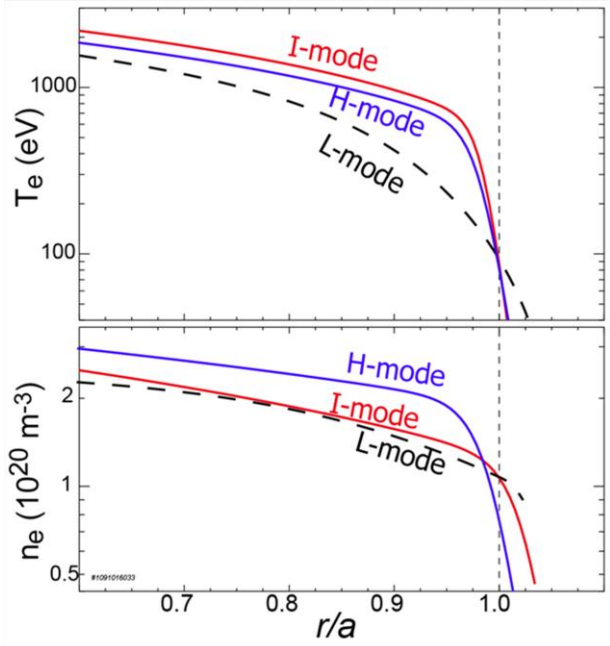

Figure 2. Comparisons of edge temperature and density profiles in L-, I- and H-mode. I-mode discharges exhibit a strong temperature pedestal, with no formation of a density pedestal.

Comparisons of temperature and density profiles in L-, I- and H-mode are shown in Figure 2.[13] The profiles are shown here for the outer 25% of the minor radius, out to just beyond the last closed flux surface. The I-mode temperature profile shows the clear formation of a strong temperature pedestal, similar in width to that seen in H-mode (typically ~3% of the normalized poloidal flux for I-mode), while the density profile illustrates almost no change from L-mode. In addition, the I-mode density profile in the scrape-off layer (SOL, r/a>1) is significantly broader than in H-mode, which is also potentially advantageous with respect to radiative divertor operation.[5] In contrast to the EDA-H-Mode, the I-mode pedestal is low collisionality, with ν* as low as 0.1.

III. EDGE FLUCTUATIONS AND PARTICLE TRANSPORT

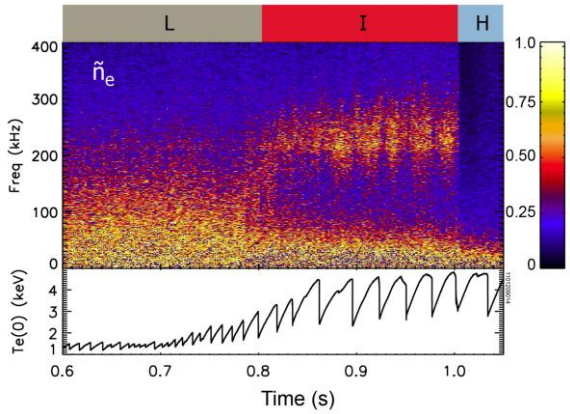

Figure 3. Time history of density fluctuation spectra from O-mode reflectometery (88Ghz). The data comes from the location of the cut-off, near r/a=0.95 for this channel during the L- and I-mode phases of this discharge. The central T_e time history is also shown.

There are clear changes in edge fluctuations in going from L-mode to I-mode.[13,14] Figure 3 shows data from O-mode reflectometry, used to measure density fluctuations near the plasma edge.[17] In the L-mode phase of this discharge, typical broadband turbulence for f < 150 kHz is present. On transition to I-mode at 0.8 s, there is a decrease in mid-frequency range turbulence (60kHz<f<150kHz), and a new,

weakly coherent mode ("WCM"), with $\delta f/f \sim 0.3$, appears at higher frequency (~250 kHz). On transition to H-mode at 1.0 s, the WCM disappears, coincident with the formation of the density pedestal. As shown in figure 4, the WCM is also seen in magnetic fluctuations measured on poloidal field pickup coils mounted outboard of the plasma on the low field side, and on Electron Cyclotron Emission (ECE) fluctuations[18]. The WCM density fluctuations are also seen with Gas Puff Imaging (GPI)[19]. When taken together, the reflectometer, ECE and GPI measurements all show that the WCM is localized to the region of the strong edge temperature gradient. In addition, GPI measurements resolve the poloidal wavenumber, giving $k_\perp \rho_S \sim 0.1$, $n_{toroidal} \sim 20$ and that the mode propagates in the electron diamagnetic direction in the plasma frame.[19] Detailed analysis of the ECE data[18] shows that the signal is dominated by temperature fluctuations, with $\delta T_e/T_e \sim 2\%$. This compares with a typical absolute density fluctuation level, from GPI measurements[18], of about 10%. Taken together, these results all point to the possibility that the WCM is the main mechanism responsible for the edge particle transport (relative to that in ELM-free H-mode) during I-mode operation. As a further test of this hypothesis, a series of experiments was performed to examine directly the relationship between density transport and the intensity of the WCM. During I-mode operation, the auxiliary heating power was ramped in steps through a range of about a factor of two. The intensity of the WCM was monitored using multiple frequencies of the reflectometry diagnostic. The majority (deuterium) particle source was determined using an analysis of absolutely calibrated D-alpha imaging near the outboard midplane. The electron loss rate is then computed, correcting for any time derivative in the plasma inventory. This approach is analogous to the technique which was used to study the effect of edge modes on particle transport in the EDA H-mode.[20] The preliminary results of one such I-mode scan show strong correlation between the particle flux and the WCM amplitude, further supporting the conjecture that there is a causative relationship between the WCM and particle transport.

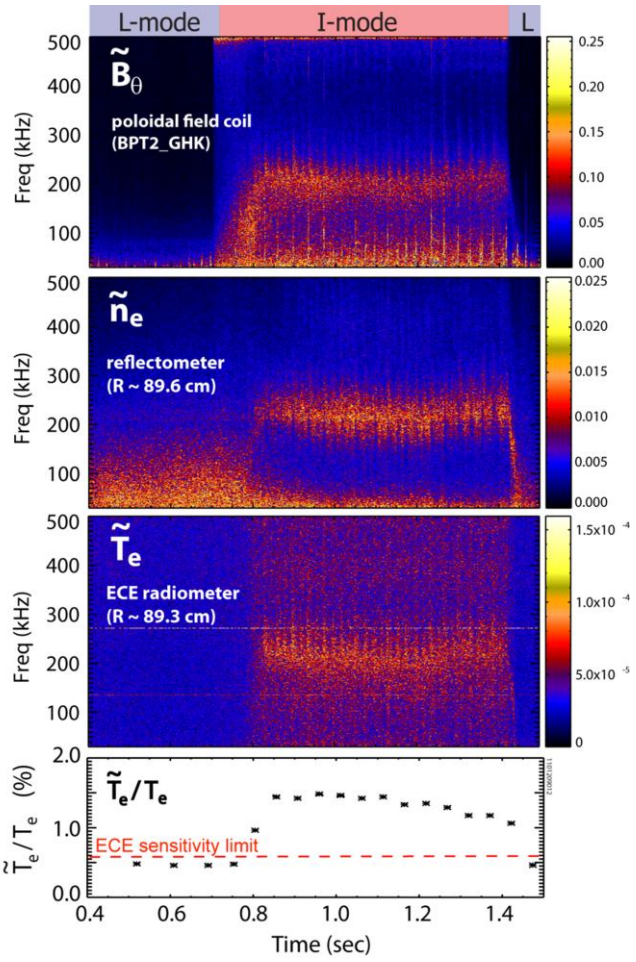

Figure 4. WCM fluctuations seen on poloidal magnetic field, density and T_e.[18]

IV. I-MODE THRESHOLD POWER

When considering extrapolation of I-mode to future experiments, including possible access on ITER, one important question is: How does the I-mode power threshold scale with plasma parameters? As a first step in trying to answer that question, a series of I-mode threshold studies was carried out on C-Mod, varying engineering parameters including toroidal field, plasma current and density. The main results are reported in reference 21, and are summarized here. For a density scan at fixed field and current, the threshold power scales approximately linearly with line average density, as shown in Figure 5. Taking the entire set over current and density, a least-squares linear regression gives a scaling of

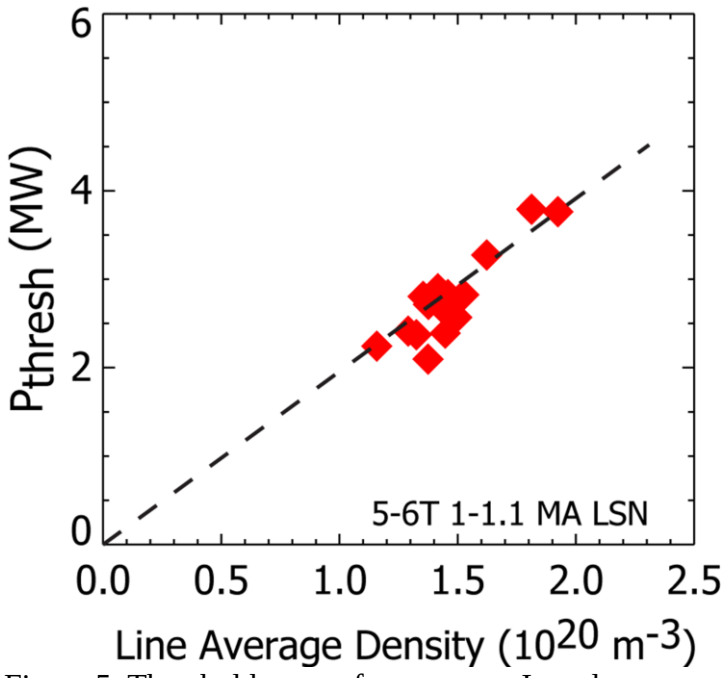

Figure 5. Threshold power for access to I-mode as a function of line average electron density. All of the data are from discharges with $\mathbf{B}\times\nabla\mathbf{B}$ away from the active X-point in lower single null, closed divertor configuration.

$$P_{th} = 2.28 I_p^{0.96} n_e^{0.52} \qquad (1)$$

However, it should be noted that there is a significant covariance between current and density in the data set. There is at most a weak dependence of P_{th} on magnetic field; for extrapolation to ITER, this dependence should not be important, since most of the C-Mod data set is obtained at the same field as is planned for ITER.

V. I-MODE POWER WINDOW AND TRANSITIONS TO H-MODE

To utilize the advantages of I-mode over the largest range of operation, it is important to

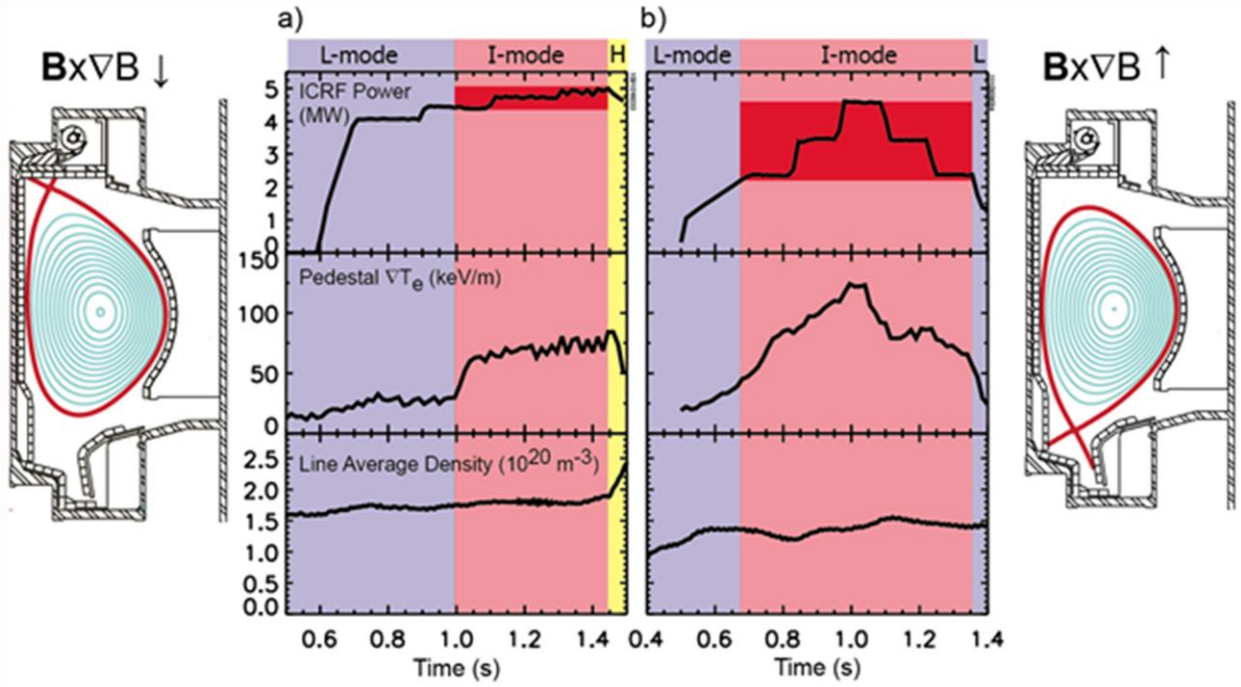

Figure 6. Comparison of I-mode power range with: a) upper single null, open divertor configuration; b) lower single null, closed vertical-plate divertor configuration.

understand the I- to H-mode transition. In many discharges with unfavorable **B**×∇B, increasing the input power in I-mode eventually leads to a transition into H-mode, with formation of the edge density transport barrier. Empirically on C-Mod, the largest power window for I-mode operation is found when the active divertor is in the closed configuration (Lower Single Null, LSN), at the bottom of the device, while, at least so far, the power window is very narrow when the active divertor is in the upper chamber (USN). Figure 6 shows a comparison of USN and LSN discharges, along with the corresponding magnetic topologies. With about a 15% increase of input power in I-mode, the USN case (Figure 6a) transitions to H-mode, while the LSN case, operating into the closed, vertical plate divertor (Figure 6b) stays in I-mode over the full range

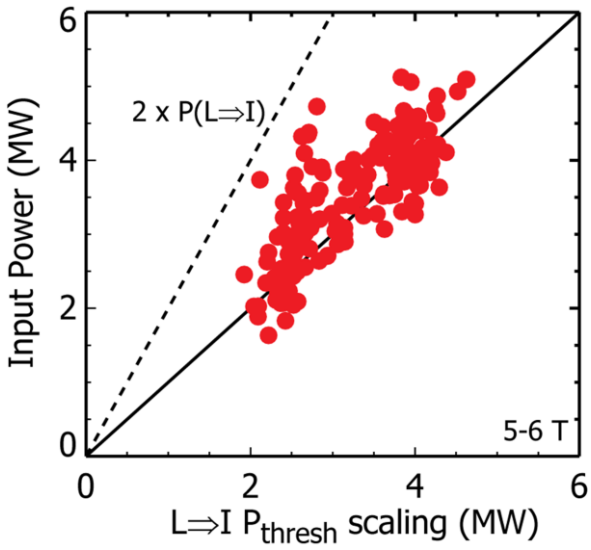

Figure 7. Power ranges for I-mode operation as a function of the threshold scaling power derived from the power law regression fit to the threshold data set (equation. 1).

of available auxiliary power. While divertor geometry is one obvious difference, other shaping parameters, in particular triangularity at the active X-point, also differ (δ_{upper}=0.67 for the USN case, δ_{lower}=0.52 for the LSN case). The importance of triangularity, as well as subtle differences in plasma density, have not been fully explored with respect to the I-mode power window, and will be the subject of future investigations. Looking at the entire data set, we find maximum ranges for the I-mode power window to be 1.5 times threshold for USN, and 1.8 times threshold for LSN. Figure 7 shows these data, including both USN and LSN cases. In many of the highest power points, there was no transition at all to H-mode, while in other cases (as in Figure 6a), the transition to H-mode can occur with only a small increment in heating power.

VI. PEDESTAL PRESSURE AND ENERGY CONFINEMENT

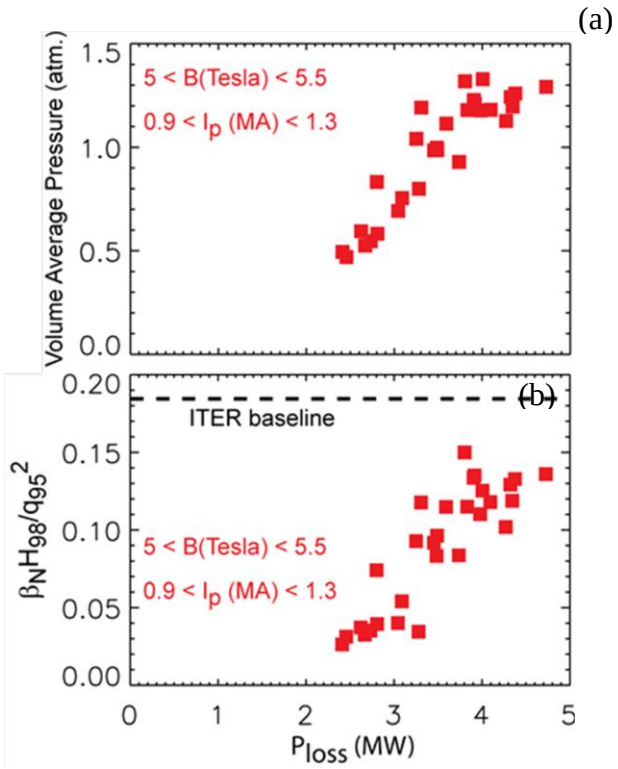

Figure 8. a)Volume average pressure as a function of $P_{loss} = P_{heat} - dW/dt$. In all cases the time derivative term is less than 10%.
b) The same data set, recast into a dimensionless fusion metric. The dashed curve shows the expected value for ITER operating in the baseline H-mode at Q=10.

Confinement scaling studies on C-Mod show that there is at most a weak confinement degradation with input power in I-mode.[13] Pedestal temperature profile measurements reveal that the width of the temperature barrier is relatively constant (~ 3% of the poloidal flux), while the height of the temperature barrier scales approximately linearly with increasing heating power. One illustration of the global confinement effect is shown in Figure 8a, which shows the linear increase in plasma pressure, as inferred from equilibrium reconstructions of β_p, as a function of heating power. This is confirmed by kinetic thermal profiles of n_e, T_e, and T_i. TRANSP[22] simulations indicate that the non-thermal ion contribution to β_p in these ICRF hydrogen minority heated discharges is usually 10% or less. Figure 8b shows the same data, plotted in terms of the dimensionless fusion metric, $\beta_N H_{98}/q^2$. In spite of its much smaller size, C-Mod, operating at the ITER field, shape and q_{95}, reaches 85% of the value on ITER required for Q=10.

VII. PEDESTAL STABILITY

Peeling-ballooning instabilities are thought to be responsible for the ELM trigger in Type-I ELMing H-mode plasmas.[23] The reduced density and pressure gradients of the I-mode pedestal, relative to H-mode, are favorable for staying below the peeling-ballooning stability boundaries. As seen in Figure 9, preliminary results using the ELITE code[24], show that the typical I-mode pedestal in C-Mod is far from both the peeling (large pedestal current), and the ballooning (large pedestal pressure gradient) boundaries. The growth rates are down by several orders of magnitude compared to those in Type-I ELMing discharges. The I-mode result indicates that there is significant headroom for increasing the I-mode pedestal pressure before the ELM boundary should be encountered.

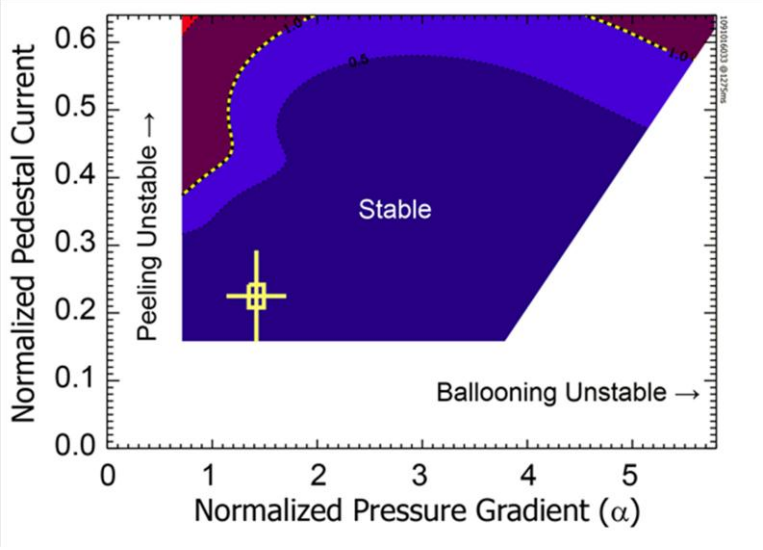

Figure 9 ELITE calculations of the peeling-ballooning growth rates for a typical I-mode pedestal.

VIII. EXTRAPOLATION TO ITER

As a first step in evaluating the possible applicability of I-mode to ITER, we have made a simple extrapolation based on observed scalings, and assumptions concerning size scaling for the I-mode threshold. Because of the significant size extrapolation from C-Mod to ITER, about a factor of 9 in linear dimension, it is clear that this part of the analysis has large uncertainty. Nevertheless, it is an instructive exercise, pointing the way for future investigations, which will undoubtedly require coordinated studies among multiple tokamaks.

C-Mod matches ITER in aspect ratio (R/a=3), B (5.3 T), q_{95} (3) shape and divertor geometry. Presuming that ITER could operate with $\mathbf{B}\times\nabla B$ away from the lower divertor, an extrapolation is made with the following assumptions:

1) $P_{L\Rightarrow I} = 1.8$ MW x $\langle n_{e,20}\rangle$ x $(S_{ITER}/S_{C\text{-}Mod})$, where S is the surface area of the last closed flux surface;
2) Match density profile shape to that seen on C-Mod ($n_0/\langle n\rangle \sim 1.3$) (though stronger peaking might obtain at ITER's lower collisionality)
3) Scale the L-mode temperature profile to force $\tau_E = \tau_{ITER89}$,[25] including alpha power in L-mode (typically 10 to 20 MW depending on density and auxiliary power;
4) Constrain $\tau_E < 1.2\ \tau_{ITER98,y2}$, $n<n_{Greenwald}$, $P_{aux}<75$ MW, $P_{L\Rightarrow I} < P_{heat} < 2\ P_{L\Rightarrow I}$, pressure at $\Psi_{95} < \Psi_{95\text{-H-mode, ITER}}$ (no ELMs);
5) Scale core and pedestal temperature profiles from C-Mod data, using

$\nabla T_{core} \propto (P_{heat}/S)^{1/2}$ (as in H-mode)

$\nabla T_{pedestal} \propto (P_{heat}/S)/n_{\Psi 95}$.

Assumption 1) is a scaling similar to that used for the L-H threshold, P~nBS, but cannot be confirmed from C-Mod data alone. The combination of core and pedestal temperature assumptions yields a global energy confinement scaling with P_{heat} consistent with the C-Mod results (section VI, above, and Reference 13). With these assumptions, the global heating power and edge density uniquely set the core temperature and density profiles, and thus the fusion performance.

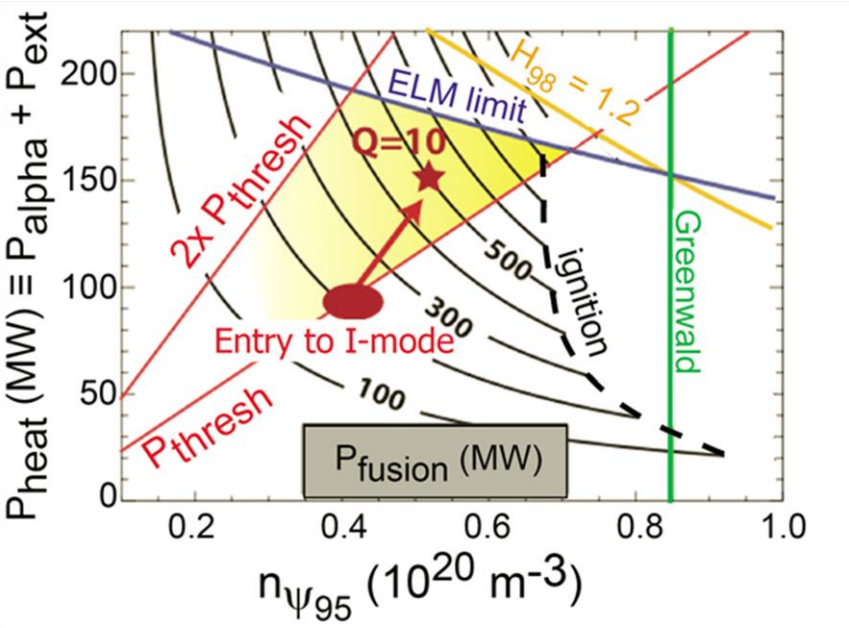

Figure 10. Contours of constant fusion power extrapolated for I-mode in ITER, as functions of heating power (apha + external), and density at the top of the temperature pedestal. The constraints on I-mode threshold power, energy confinement, the density limit, and the ELM pressure limit are shown by the straight lines. According to the assumptions made in this extrapolation, I-mode operation would be accessible in the shaded region. The Q=10 operation point is shown by the solid star, and ignition (P_{ext}=0) would be reached at the dashed line to the right.

The results of this exercise are summarized in Figure 10. The contour plot shows lines of constant fusion power. Under the assumptions, I-mode should be accessible from L-mode with available auxiliary power at line average density of about $5x10^{19}$ m^{-3}, or with progressively less power as the target density is decreased. In I-mode, alpha heating takes over, and fusion power is controlled mainly through density control. The nominal Q=10 operation point is shown on the plot, and appears to be feasible without pushing to the pedestal/ELM stability limit. Initial attempts to simulate I-mode conditions for ITER with the TSC model[26], give similar results: I_p = 14 MA, n/n_g = 0.75, n(0)/<n>=1.36, P_{aux}=40 MW, T_{ped} = 4 keV, T_0 = 22 keV, H_{98} = 1, P_{alpha} = 90 MW, P_{fusion} = 450 MW (Q=11).

IX. SUMMARY

I-mode is a promising regime of operation for the tokamak, combining many favorable characteristics, including: good energy confinement with particle and impurity control; no need for large intermittent edge instabilities (such as ELMs) to regulate the pedestal particle transport; demonstrated stationary operation; weak energy confinement degradation with increasing input power; balanced inner and outer divertor power loading in the single null configuration; peeling-ballooning stable pedestal. Candidate fluctuations have been identified which are always present during I-mode, and there is mounting (but still circumstantial) evidence that they are responsible for the enhanced particle and impurity transport across the pedestal, relative to that seen in the inter-ELM phase of H-mode. A preliminary examination of I-mode application ITER, based on simple scalings, is promising and points the way for future experiments.

There is clearly still much to be learned about the I-mode regime. Future investigations will be important to understand further the dynamics of the I-mode pedestal, and possible application of I-mode to burning plasma experiments. Open questions include: What is the underlying nature of the WCM fluctuations? How are energy and particle transport decoupled? Can the L- to I-mode power threshold be lowered? What determines the I- to H-mode transition, and how can H-mode be best avoided at high input power? How do the thresholds and performance scale (particularly with plasma size)? Many of these questions can only be answered through coordinated experiments across multiple tokamak facilities; some of these are already in the planning stages, coordinated under the auspices of the International Tokamak Physics Activity (ITPA).

References:

[1]D.N. Hill, Journal of Nuclear Materials, v 241-243 (1997)182.

[2]F. Wagner, Fussmann, G.; Grave, T.; Keilhacker, M.; Kornherr, M.; Lackner, K.; McCormick, K.; Muller, E.R.; Stabler, A.; Becker, G.; Bernhardi, K.; Ditte, U.; Eberhagen, A.; Gehre, O.; Gernhardt, J.; von Gierke, G.; Glock, E.; Gruber, O.; Haas, G.; Hesse, M.; Janeschitz, G.; Karger, F.; Kissel, S.; Kluber, O.; Lisitano, G.; Mayer, H.M.; Meisel, D.; Mertens, V.; Murmann, H.; Poschenrieder, W.; Rapp, H.; Rohr, H.; Ryter, F.; Schneider, F.; Siller, G.; Smeulders, P.; Soldner, F.; Speth, E.; Steuer, K.-H.; Szymanski, Z.; Vollmer, O., Physical Review Letters, v 53(1984)1453.

[3]M. Shimada, D.J. Campbell, V. Mukhovatov, M. Fujiwara, N. Kirneva, K. Lackner, M. Nagami, V.D. Pustovitov, N. Uckan, J. Wesley, N. Asakura, A.E. Costley, A.J.H. Donné, E.J. Doyle, A. Fasoli, C. Gormezano, Y. Gribov, O. Gruber, T.C. Hender, W. Houlberg, S. Ide, Y. Kamada, A. Leonard, B. Lipschultz, A. Loarte, K. Miyamoto, V. Mukhovatov, T.H. Osborne, A. Polevoi and A.C.C. Sips, Nuclear Fusion 47 (2007) S1.

[4]A.W. Leonard, Herrmann, A.; Itami, K.; Lingertat, J.; Loarte, A.; Osborne, T.H.; Suttrop, W. Journal of Nuclear Materials, v 266-269(1999)109.

[5]A. Loarte, B. Lipschultz, A.S. Kukushkin, G.F. Matthews, P.C. Stangeby, N. Asakura, G.F. Counsell, G. Federici, A. Kallenbach, K. Krieger, A. Mahdavi, V. Philipps, D. Reiter, J. Roth, J. Strachan, D. Whyte, R. Doerner, T. Eich, W. Fundamenski, A. Herrmann, M. Fenstermacher, P. Ghendrih, M. Groth, A. Kirschner, S. Konoshima, B. LaBombard, P. Lang, A.W. Leonard, P. Monier-Garbet, R. Neu, H. Pacher, B. Pegourie, R.A. Pitts, S. Takamura, J. Terry, E. Tsitrone and the ITPA Scrape-off Layer and Divertor Physics Topical Group, Nuclear Fusion 47(2007)S203.

[6]T.E. Evans, Fenstermacher, M.E.; Moyer, R.A.; Osborne, T.H.; Watkins, J.G.; Gohil, P.; Joseph, I.; Schaffer, M.J.; Baylor, L.R.; Becoulet, M.; Boedo, J.A.; Burrell, K.H.; deGrassie, J.S.; Finken, K.H.; Jernigan, T.; Jakubowski, M.W.; Lasnier, C.J.; Lehnen, M.; Leonard, A.W.; Lonnroth, J.; Nardon, E.; Parail, V.; Schmitz, O.; Unterberg, B.; West, W.P., Nuclear Fusion, v 48(2008)024002.

[7]A. Kirk, Nardon, E.; Akers, R.; Be´coulet, M.; De Temmerman, G.; Dudson, B.; Hnat, B.; Liu, Y.Q.; Martin, R.; Tamain, P.; Taylor, D. Source: Nuclear Fusion, v 50(2010)034008.

[8]P.T. Lang, G.D. Conway, T. Eich, L. Fattorini, O. Gruber, S. Günter, L.D. Horton, S. Kalvin, A. Kallenbach, M. Kaufmann, G. Kocsis, A. Lorenz, M.E. Manso, M. Maraschek, V. Mertens, J. Neuhauser, I. Nunes, W. Schneider, W. Suttrop, H. Urano and the ASDEX Upgrade Team, Nuclear Fusion 44(2004)665.

[9]E.J. Doyle, Baylor, L.R.; Burrell, K.H.; Casper, T.A.; DeBoo, J.C.; Ernst, D.R.; Garofalo, A.M.; Gohil, P.; Greenfield, C.M.; Groebner, R.J.; Hyatt, A.W.; Jackson, G.L.; Jernigan, T.C.; Kinsey, J.E.; Lao, L.L.; Lasnier, C.J.; Leboeuf, J.-N.; Makowski, M.; McKee, G.R.; Moyer, R.A.; Murakami, M.; Osborne, T.H.; Peebles, W.A.; Porkolab, M.; Porter, G.D.; Rhodes, T.L.; Rost, J.C.; Rudakov, D.; Staebler, G.M.; Stallard, B.W.; Strait, E.J.; Sydora, R.D.; Synakowski, E.J.;

Wade, M.R.; Wang, G.; Watkins, J.G.; West, M.P.; Zeng, L. Source: Plasma Physics and Controlled Fusion, v 43, n 12A, p A95-A112, Dec. 2001

[10]M. Greenwald, M. (Plasma Fusion Center, MIT, Cambridge, MA, USA); Boivin, R.; Bonoli, P.; Fiore, C.; Goetz, J.; Granetz, R.; Hubbard, A.; Hutchinson, I.; Irby, J.; Lin, Y.; Marmar, E.; Mazurenko, A.; Mossessian, D.; Pedersen, T.S.; Rice, J.; Snipes, J.; Schilling, G.; Taylor, G.; Terry, J.; Wolfe, S.; Wukitch, S. Source: Plasma Physics and Controlled Fusion, v 42, suppl.5A, p A263-9, May 2000

[11]F. Ryter, W.Suttrop, B.Brusehaber, M.Kaufmann ,V.Mertens, H.Mur-mann, A.G.Peeters, J.Stober, J.Schweinzer, H.Zohm, and ASDEX Upgrade Team, Plasma Phys. Controlled Fusion 40,(1998)725.

[12]R.M. McDermott, Lipschultz, B.; Hughes, J.W.; Catto, P.J.; Hubbard, A.E.; Hutchinson, I.H.; Granetz, R.S.; Greenwald, M.; Labombard, B.; Marr, K.; Reinke, M.L.; Rice, J.E.; Whyte, D. Source: Physics of Plasmas, v 16, n 5, 2009

[13]D.G. Whyte, Hubbard, A.E.; Hughes, J.W.; Lipschultz, B.; Rice, J.E.; Marmar, E.S.; Greenwald, M.; Cziegler, I.; Dominguez, A.; Golfinopoulos, T.; Howard, N.; Lin, L.; McDermottb, R.M.; Porkolab, M.; Reinke, M.L.; Terry, J.; Tsujii, N.; Wolfe, S.; Wukitch, S.; Lin, Y. Source: Nuclear Fusion, v 50, n 10, October 2010

[14]A.E. Hubbard, Whyte, D.G.; Churchill, R.M.; Cziegler, I.; Dominguez, A.; Golfinopoulos, T.; Hughes, J.W.; Rice, J.E.; Bespamyatnov, I.; Greenwald, M.J.; Howard, N.; Lipschultz, B.; Marmar, E.S.; Reinke, M.L.; Rowan, W.L.; Terry, J.L. Source: Physics of Plasmas, 18(2011), n 5

[15]N.T. Howard, Greenwald, M.; Rice, J.E. Source: Review of Scientific Instruments, 82(2011)033512.

[16]B. Lipschultz, Lin, Y.; Marmar, E.S.; Whyte, D.G.; Wukitch, S.; Hutchinson, I.H.; Irby, J.; LaBombard, B.; Reinke, M.L.; Terry, J.L.; Wright, G. Source: Journal of Nuclear Materials, v 363-365(2007)1110.

[17]N.P. Basse, N.P., Edlund, E.M.; Ernst, D.R.; Fiore, C.L.; Greenwald, M.J.; Hubbard, A.E.; Hughes, J.W.; Irby, J.H.; Lin, L.; Lin, Y.; Marmar, E.S.; Mossessian, D.A.; Porkolab, M.; Rice, J.E.; Snipes, J.A.; Stillerman, J.A.; Terry, J.L.; Wolfe, S.M.; Wukitch, S.J.; Zhurovich, K.; Kramer, G.J.; Mikkelsen, D.R. Source: Physics of Plasmas, 12(2005)52512.

[18]A.E. White, Phillips, P.; Whyte, D.G.; Hubbard, A.E.; Sung, C.; Hughes, J.W.; Dominguez, A.; Terry, J.; Cziegler, I. Source: Nuclear Fusion, 51(2011)113005.

[19]I. Cziegler, Terry, J.L.; Hughes, J.W.; LaBombard, B. Source: Physics of Plasmas, 17(2010)056120.

[20]J.L. Terry, N.P. Basse, I. Cziegler, M. Greenwald, O. Grulke, B. LaBombard, S.J. Zweben, E.M. Edlund, J.W. Hughes, L. Lin, Y. Lin, M. Porkolab, M. Sampsell, B. Veto and S.J. Wukitch, Nuclear Fusion 45(2005)1321.

[21]A E Hubbard, D G Whyte, A Dominguez, J W Hughes, Y Ma, E S Marmar, Y Lin, M L Reinke, *Threshold conditions for transitions to I-mode and H-mode with unfavourable ion drift direction*, submitted to Nuclear Fusion, 2011.

[22]R.V. Budny, M.G. Bell, A.C. Janos, D.L. Jassby, L.C. Johnson, D.K. Mansfield, D.C. McCune, M.H. Redi, J.F. Schivell, G. Taylor, T.B. Terpstra, M.C. Zarnstorff and S.J. Zweben, Nuclear Fusion 35(1995)1497.

[23]P.B. Snyder, Wilson, H.R.; Ferron, J.R.; Lao, L.L.; Leonard, A.W.; Osborne, T.H.; Turnbull, A.D.; Mossessian, D.; Murakami, M.; Xu, X.Q. Source: Physics of Plasmas, v 9 (2002) 2037.

[24]P.B. Snyder, Burrell, K.H.; Wilson, H.R.; Chu, M.S.; Fenstermacher, M.E.; Leonard, A.W.; Moyer, R.A.; Osborne, T.H.; Umansky, M.; West, W.P.; Xu, X.Q. Source: Nuclear Fusion, 47(2007), 961.

[25]E.J. Doyle, W.A. Houlberg, Y. Kamada, V. Mukhovatov, T.H. Osborne, A. Polevoi, G. Bateman, J.W. Connor, J.G. Cordey (retired), T. Fujita, X. Garbet, T.S. Hahm, L.D. Horton, A.E. Hubbard, F. Imbeaux, F. Jenko, J.E. Kinsey, Y. Kishimoto, J. Li, T.C. Luce, Y. Martin, M. Ossipenko, V. Parail, A. Peeters, T.L. Rhodes, J.E. Rice, C.M. Roach, V. Rozhansky, F. Ryter, G. Saibene, R. Sartori, A.C.C. Sips, J.A. Snipes, M. Sugihara, E.J. Synakowski, H. Takenaga, T. Takizuka, K. Thomsen, M.R. Wade, H.R. Wilson, ITPA Transport Physics Topical Group, ITPA Confinement Database and Modelling Topical Group and ITPA Pedestal and Edge Topical Group, Nuclear Fusion 47(2007)S18.

[26]S.C. Jardin, Pomphrey, N.; Delucia, J., J. Comput. Phys. 66(1986)481.